Advances in Reliability, Safety and Security, Part 10 – Kołowrocki, Kosmowski (eds.)
 ISBN 978-83-68136-22-7 (printed), ISBN 978-83-68136-09-8 (electronic)

Advances in Reliability, Safety and Security

ESREL 2024
Monograph Book Series

Failure And Repair Rates For Lane Detection For Safety Assessment Of Autonomous Driving From CARLA Simulation

Ivo Häring, Rachana Padariya, Georg Vogelbacher, Fabian Höflinger, Alexander Richter, Jörg Finger, Aishvarya Kumar Jain, Mirjam Fehling-Kaschek

Fraunhofer EMI, Freiburg, Germany

Abstract

In the tremendously developing field of autonomous driving (AD), it is of utmost importance that system functions are safe. This paper offers a method for evaluating AD sub-systems' safety, with an emphasis on lane detecting subsystems in a range of environmental settings. CARLA simulation platform is used to determine the failure rate of a lane-detecting software algorithm provided by CARLA itself. The approach shows that lane detection reliability depends critically on environmental factors, particularly on precipitation levels. Results were generated from video analysis of 180 s of autonomous driving using inspections for every 5 s by utilizing different failure rate definitions that considered fractions of failure observations, number of failure sequences, including with various minimum lengths. Failure rate per time definitions are identified which are most consistent, namely considering the number of failure sequences observed divided by time span length while considering duration times. However, better consistent with the present data is to use failure and repair rates assuming exponential failure and repair models. Repair time distributions from CARLA simulation were used to determine mean time to repair empirically for the rain levels 0%, 25%, 75% and 100%. It is found that already within 180 s of simulation the failure probability is very close to the asymptotic failure probability as expected from a two state Markov model. The methodologies and first results of the present work are deemed relevant for the development and assessment of safety-critical autonomous driving subsystems. It is evident that shorter inspection intervals, much longer observation intervals and more environmental scenario parameters could be used for Markov state space refinement or extension. It is expected that these extensions would improve the precision of, e.g., exponential failure rate and repair models and more advanced time-dependent failure and repair models, e.g. Weibull models.

Keywords: CARLA simulator, autonomous driving, lane detection, object detection, Markov model, failure rate per time, failure probability, repair or recovey rate, safety and reliability analysis, functional safety (ISO 26262), safety of the intended functionality (SOTIF, ISO 21448), Markov state space expansion and contraction, urban driving scenario.

1. Introduction

Markov modelling and simulation for safety assessment of autonomous driving (AD) functions is a promising approach on system level, as it allows explainable insight in overall system availability, reliability, fail operational, fail safe, fail emergency, and failure behavior. However, classical Markov simulations are limited and challenging (Horeis et al. 2020), thus requiring extensions. One issue to overcome is the need for a sufficiently broad overall system definition (generalized Markov state space) that needs to include environment information covering street and weather scenario (street geometry and conditions, weather, time-of-the-day), driver and occupants, other road users as well as the technical system (sensors, hardware, software, interfaces, cloud services, car-to-X communication). Examples of overall Markov models for AD considering technical system and driver are given in (Nyberg, 2018) and considering in addition environment are given in (Satsrisakul 2018) (Häring et al. 2022).

Along with overall Markov state space definition for AD comes the insight that failure rates are in general time-dependent, e.g., due to aging, depend on environmental conditions, e.g., sensor performance during sun glare, strong rain or fog versus bright cloudy day conditions, and may be influenced by further external boundary conditions, e.g., varying external support services regarding location and traffic conditions, or be influenced by

systemic behavior, e.g., connectivity or software updating and improvement over time. Hence, classical homogenous Markov models are not sufficient, also inhomogeneous time dependent models do not suffice, since the above examples require to cover state condition-based transition models. To overcome this challenges requires the use of overall state space informed continuous time dependent simulations that can digest discontinuities or even Monte Carlo Markov models (Satsrisakul, 2018) (Horeis et al. 2020) (Häring et al. 2022) (Häring et al. 2023b). For the latter also see application examples reviewed in (Riedmaier et al. 2020) and regarding AD implementation in (Zhu et al. 2022). Further extension options include hierarchical semi-Markov processes (Mattsson 2020) and related state transition characteristics (Fenoaltea, 2022).

Another challenge is state space explosion for realistic system resolutions requiring large computational resources and implying the need to scale state space, i.e. to adopt modelling resolution to avoid state space explosion. Options include so summarize states and to define subsystems or subfunctions for which substitute or ersatz Markov models are provided (Puig Walz et al. 2023). Another option is to define state space expanding and contracting models that preserve conservation of total probability flow as given in (Pouya and Madni, 2021) (Pouya and Madni, 2022) for AD operation implementation and in (Häring et al. 2023a) for system safety analysis. Subsystems can also be simulated (Rinaldo and Horeis, 2020) to provide input to Markov models.

Another main issue and the focus of the present paper is the lack of failure rate and repair data for advanced Markov Simulation data (Richter et al. 2023). An option is to consider very short simulation sequences and to use metrics form computer vision such as false positive and false negative along with scenario data to determine simple failure rate models from AD simulation (Häring et al. 2024). The present approach considers a time span of 3 minutes AD in a predefined city environment to assess lane detection and is based on (Padariya, 2024).

The paper continues with section 2 describing further related research. Section 3 gives details of the implementation and quantitative evaluation used to compute failure and repair (recovery) rates. It also shows how Markov modeling can include non-ego-car factors, i.e. environmental external factors. Section 4 presents results, mainly different failure rates based on different definitions. Failure and repair rates from simulation are presented. Finally, asymptotic distributions of probabilities are determined using an elementary Markov model and compared with pure simulation data and discussed. Section 5 gives summary and conclusions.

2. State of the art, gaps and own approach

There is an increasing number of Real-world datasets. They include Cityscapes (Cordts et al. 2026) (Breitenstein and Fingscheidt, 2022), Berkeley DeepDrive (Xu et al. 2017), KITTI (Karlsruhe Institute of Technology and Toyota Technological Institute) dataset (Geiger et al. 2013), the nuTonomy scenes (nuScenes) dataset covering the full autonomous vehicle sensor suite: 6 cameras, 5 radars and 1 lidar, all with full 360 degree field of view (Caesar et al. 2020) and similar data by the A*3D dataset with focus on Lidar and night data, and the dataset of annotated DAVIS (dynamic and active-pixel vision sensors) driving recordings (DDD17) (Binas et al. 2017) (Chamain et al. 2022) and DDD20 (Hu et al. 2020) focusing on human behavior have been widely utilized for this purpose. Data can be also collected for critical scenarios only (Häring et al. 2021).

However, as argued in (Häring et al. 2024), CARLA (CAR Learning to Act) (Dosovitskiy et al. 2017) (CARLA 2024), CARLA (CAR Learning to Act) is one of the leading AD simulation environments (Huang et al. 2016), in particular for the urban domain (Coelho and Oliveira, 2022) and regarding sensor simulations (Rosique et al. 2019). It can be used instead of real world data or data acquisition for pre-assessment of safety and of safety of the intended functionality of AD functions. It is an open-source layer over Unreal Engine 4 (UE4) (El-Wajeh et al. 2022; Malik et al. 2022). It covers AD development, testing and validation (Berlincioni, 2022).

The Operational Design Domain (ODD) is the lane detection sub-function for a credible range of environmental and operational factors, in particular in urban areas. Simulation options are varied over a wide range of parameters, including statistical generation of active road participants, i.e. spawning of objects. The article presents several quantitative approaches to generate failure and repair rates from CARLA simulation for lane detection. Focus is on different failure rate expressions and the discussion results and their comparison. Finally, recommendations are given regarding selection of approach for the application case Markov simulation with constant failure and repair rates dependent on influencing factors such as precipitation, fog, time of the day/sun position.

3. Methodology and implementation details

3.1 Failure and repair rates and mean times to X from continuous failure and repair time simulation data

Failure rate is a measure of how often a system or component fails within a given period of time. It is expressed as the number of failures per unit of time, e.g. (Finkelstein, 2008) (Goble, 2010) (Rausand, 2014) (Verma et al.

2016) (Birolini, 2017). Failure rate is generally used to evaluate the reliability of a system or of components, and to estimate the likelihood of failures in the future.

In formal notation, failure probability of a system or component is defined as the probability at which it fails within a given period of time $[0, t]$. Failure probability corresponds to the cumulative failure probability $F(t)$ based on a failure probability density function (PDF) $f(t)$, i.e. $F(t) = \int_{t_0=0}^{t} f(\tau)d\tau$. From this, a failure rate $r(t) \equiv z(t) = \frac{f(t)}{R(t)}$ can be computed using the reliability probability $R(t) = 1 - F(t)$. The failure rate is the failure rate per time at time at time t that the system fails assuming it has not failed until time t. The notation introduced in this text paragraph allows to define the random variable failure time T with expectation value $E[t] = \int_0^{\infty} f(\tau)\tau \, d\tau$.

Assuming an exponential distribution for the failure time random variable of an AD function results in

$F(t) = \int_{t_0=0}^{t} f(\tau)d\tau = 1 - e^{-\lambda t}$, failure probability, approaching 1 as time increases, (1)

$R(t) = 1 - F(t) = e^{-\lambda t}$, non-failure or reliability probability, approaching 0 as time increases,

$f(t) = \frac{d}{dt}F(t) = \lambda e^{-\lambda t}$, failure probability density,

$r(t) = \frac{f(t)}{R(t)} = \lambda = const. > 0$, failure rate,

where failure probability increases with time and non-failure probability or reliability decreases with time.

Using the repair rate μ results in similar expressions for the repair time random variable T_r of an AD function when again assuming an exponential distribution. However, this time, repair probability increases with time and non-repair probability decreases with time:

$F_r(t) = \int_{t_0=0}^{t} f_r(\tau) \, d\tau = 1 - e^{-\mu t}$, repair probability, approaching 1 as time increases, (2)

$R_r(t) = 1 - F_r(t) = e^{-\mu t}$, non-repair probability or probability of being not repaired, approaching 0 as time increases,

$f_r(t) = \frac{d}{dt}F_r(t) = \mu e^{-\mu t}$, repair probability density,

$r_r(t) = \frac{f_r(t)}{R_r(t)} = \lambda = const. > 0$, repair rate.

Mean time to failure (MTTF) and mean time to repair (MTTR) are computed using expectation values or first moments of the failure and repair density, respectively, i.e. expectation values of the operation time and repair time random variables. Mean time to failure can also be expressed as averaging over the reliability probability. Mean time to repair similarly can be expressed by averaging over the non-repair probability (complement of repair probability). In detail:

$MTTF = E_f[t] = \int_{t_0=0}^{\infty} f(\tau)\tau \, d\tau = \int_{t_0=0}^{\infty} R(t)d\tau$, Mean time to failure, (3)

$MTTR = E_{f_r}[t] = \int_{t_0=0}^{\infty} f_r(\tau)\tau \, d\tau = \int_{t_0=0}^{\infty} R_r(\tau)d\tau$, Mean time to repair.

For the last equality sign in the first row of (3) consider for partial integration the expression $\frac{d(R(\tau)\tau)}{d\tau} = \frac{d(R(\tau))}{d\tau}\tau + R(\tau) = \frac{d(1-F(\tau))}{d\tau}\tau + R(\tau) = -\frac{dF(\tau)}{d\tau}\tau + R(\tau) = -f(\tau)\tau + R(\tau)$ using (1) and solve for $f(\tau)\tau = R(\tau) - \frac{d(R(\tau)\tau)}{d\tau}$. This can be used to compute (see (Rausand and Haugen 2020) p. 560)

$MTTF = E_f[t] = \int_{t_0=0}^{\infty} f(\tau)\tau \, d\tau = \int_0^{\infty} \left(R(\tau) - \frac{d(R(\tau)\tau)}{d\tau}\right) d\tau = \int_0^{\infty} R(\tau) \, d\tau - R(\tau)\tau|_0^{\infty} = \int_0^{\infty} R(\tau) \, d\tau.$ (4)

The last equation holds when assuming $\lim_{\tau\to 0} R(\tau)\tau = 0$ and $\lim_{\tau\to\infty} R(\tau)\tau = 0$, which is reasonable since $R(0) = 1$ and $R(\tau)$ can be assumed to decrease faster than τ increases. In a similar way one has

$MTTR = E_{f_r}[t] = \int_{t_0=0}^{\infty} f_r(\tau)\tau \, d\tau = \int_0^{\infty} \left(R_r(\tau) - \frac{d(R_r(\tau)\tau)}{d\tau}\right) d\tau = \int_0^{\infty} R_r(\tau) \, d\tau - R_r(\tau)\tau|_0^{\infty} =$
$\int_0^{\infty} R_r(\tau) \, d\tau.$ (5)

as the non-repair probability vanishes in $\lim_{\tau\to\infty} R_r(\tau)\tau = 0$.

In case of an exponential distribution, starting from the definition $MTTF = E_f[t] = \int_{t_0=0}^{\infty} f(\tau)\tau \, d\tau = \int_0^{\infty} \lambda e^{-\lambda\tau}\tau \, d\tau$, using the substitution $x = \lambda\tau$, $\frac{dx}{d\tau} = \lambda$, $d\tau = \frac{dx}{\lambda}$ results in $MTTF = \int_0^{\infty} xe^{-x}\frac{dx}{\lambda} = \frac{1}{\lambda}\int_0^{\infty} xe^{-x}dx = \frac{1}{\lambda}$. The last equality is obtained from the general integral

expression with an exponential function $\int_0^\infty x^n e^{-ax} dx = \Gamma(n+1)/a^{n+1}$ for $n = 1$ and $a = 1$ as $\Gamma(2) = 1$, i.e. $\int_0^\infty xe^{-x} dx = \Gamma(2) = 1$ (see, e.g. (Musiol et al. 1995) p. 939 and p. 946).

Regarding simulation data, for high resolution, the following data can be assumed to be available for $t_0 = 0 < t_1 < t_2 < \cdots < t_N$, where each point in time is marking a switch from operational to fail or from fail to operational while starting with operational or failed. Figure 1 shows the first case. Operation time durations shown are $t_1 - t_0, t_3 - t_2, t_5 - t_4$ and repair times shown are $t_2 - t_1, t_4 - t_3, t_6 - t_5$. From this the mean simulation-based time to failure can be computed as

$$MTTF_{sim} = \frac{1}{\sum_{i=0}^{N-1}(i \text{ is even})_{lb}} \sum_{i=0}^{N-1}(t_{i+1} - t_i)(i \text{ is even})_{lb} = \frac{1}{\lambda}, \tag{6}$$

where the logic bracket $(A)_{lb} = 1$ if A is true and 0 if A is false. The simulation-based mean time to repair reads

$$MTTR_{sim} = \frac{1}{\sum_{i=1}^{N-1}(i \text{ is odd})_{lb}} \sum_{i=1}^{N-1}(t_{i+1} - t_i)(i \text{ is odd})_{lb} = \frac{1}{\mu}. \tag{7}$$

For large simulation times and a large number of failures one expects that $\sum_{i=0}^{N-1}(i \text{ is even})_{lb} \approx \sum_{i=1}^{N-1}(i \text{ is odd})_{lb} \approx \frac{N}{2}$. Note that the last equality in equations (6) and (7) only hold in case of an exponentially distributed failure and repair time as described in equations (1) and (2). Note that (6) and (7) can be evaluated in the same way, if the transition times have been determined from regular time-equidistant inspection. However, as resolution decreases the deviation between the correct version of the two equations with arbitrary transition points in time and equidistant points in time increases.

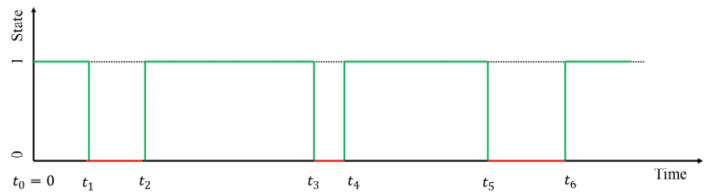

Fig. 1. Markov chain with repair for autonomous lane detection starting in operational state. Green horizontal lines are sample operation time intervals and red horizontal lines are sample repair operation times.

Furthermore, equations (6) and (7) assume that the failure points in time and the repair points in time can be determined exactly. In practice it is easier to inspect the lane or object detection system at regular short enough equidistant time intervals to determine if AD functionality is operational.

3.2 CARLA simulator und lane detection algorithms used

The CARLA simulation data used is detailed in Table 1.

Table 1. CARLA scenario parameter option ranges used for the generation of the simulations. Based in parts on CARLA API (Application Programming Interface) description (Python API - CARLA Simulator 2023).

Parameter category	Parameter	Value range/type
Weather conditions	Cloudiness	0 (clear) - 100 (overcast)
	Precipitation	0 (none) - 100 (heavy)
	Wind intensity	0 (calm) - 100 (stormy)
	Sun azimuth (from perspective of ego car)	0 - 360 degrees (position of sun in the sky)
	Sun altitude	-90 (sunrise/sunset) - 90 degrees (overhead)
	Fog density	0 (clear) - 100 (dense fog): Chosen 0 - 0
	Fog distance	Distance in meters where fog starts to appear
	Wetness	0 (dry) - 100 (wet)
Lighting and time	Time of day	0 - 24 (hour format)
Traffic control	Traffic light state	Green, Yellow, Red
Road geometry	Lane width	Varies (in meters)
	Number of lanes	Varies (in any number)
Vehicles and traffic	Vehicle types	Sedan, SUV, Truck, etc.
	Vehicle speed	Varies (in km/h or mph)
Scenarios	Urban, highway, rural, etc.	Custom scenarios based on the above parameters
Town	Town names	(e.g., Town01, Town02, Town03, Town04, Town05, Town06, Town07, Town10 in CARLA)
Pedestrians	Total number of pedestrians in scenario	70; total number of pedestrians in Town05

3.3 Asymptotic probabilities of being in operational and failed states using failure and repair rates

Another elementary evaluation is to determine the asymptotic probability distribution between operational and failed states using assuming a two state model, where state 0 is operational state and state 1 is failed state. In this case we have for the probabilities of being in sate 0 and state 1, respectively (see e.g. (Rausand 2011), p. 309, (Gupta et al. 2015) (Duer et al. 2023)),

$$p_0(t) = \frac{\mu}{\lambda+\mu} + \frac{\lambda}{\lambda+\mu} e^{-(\lambda+\mu)t}, \;\; p_1(t) = \frac{\lambda}{\lambda+\mu} - \frac{\lambda}{\lambda+\mu} e^{-(\lambda+\mu)t} \tag{8}$$

and for asymptotically large times we find

$$\lim_{t\to\infty} p_0(t) = \frac{\mu}{\lambda+\mu} = \frac{\frac{1}{MTTR}}{\frac{1}{MTTF}+\frac{1}{MTTR}} = \frac{MTTF}{MTTR+MTTF}, \;\; \lim_{t\to\infty} p_1(t) = \frac{\lambda}{\lambda+\mu} = \frac{MTTR}{MTTR+MTTF}. \tag{9}$$

4. Results and Discussion

4.1. CARLA sample simulation results

Table 2 shows sample operational and failure event of lane detection in CARLA simulation evaluated from a driving sequence of 180 s.

Table 2. Failure of lane detection within CARLA for different rain intensities and road geometries. The table notes street geometry (straight, curve, intersection) at inspection of performance of lane detection. Inspection takes place every 5 seconds at 0 s, 5 s, 10 s, …, 180 s.

	Cityside Road Scenario											
% of rain	0% rain			25% rain			75% rain			100% rain		
Time [s]	straight	curve	intersection	straight	curve	intersection	straight	curve	intersection	straight	curve	intersection
0												
5									x x x x			
10						x x x			x	x x x x		
15						x x			x x x			x
20			x x x			x x	x x					x x x
25												x x
30			x x x			x x		x x x x		x x		
35				x x x				x				
40			x x x x	x				x x x			x x x	
45		x			x x x x		x x					x
50		x x x			x							x x
55		x x							x x x			x x x
60 (1min)						x x x			x			x
5						x						
10			x x						x x x x		x x x x	
15			x x						x		x	
20			x x x			x x x			x x x			x x x
25						x		x x				x x
30												x x
35	x x						x x x					
40					x x x							
45			x x x		x			x x		x x		
50								x x x				
55				x x x				x				x x x
120 (2min)		x x										
5							x x x					x x x
10						x x			x x			x x
15		x x				x x			x x		x x	
20		x		x x							x x x	
25						x x			x x			
30	x x x								x x x	x x x		
35					x x x				x			x x x
40			x x		x x							x
45			x x x		x x						x x x	
50			x					x x x				x
55					x x							x x
180 (3min)												
No.of crosses	2	6	10	4	8	11	4	7	13	4	6	17
No.of red crosses	2	2	6	1	3	5	2	3	4	3	2	2
No.of blue crosses	2	2	7	1	4	6	4	4	4	3	4	5
No.of violet crosses	1	2	7	3	4	4	2	3	7	2	3	8
No.of orange crosses	0	1	3	1	2	2	0	3	6	2	4	5
Total no.of crosses	18			25			25			27		
Total no.of red crosses	10			9			9			7		
Total no.of blue crosses	11			11			16			12		
Total no.of violet crosses	10			11			12			13		
Total no.of orange crosses	4			5			9			11		

4.2. Failure and repair rates from empirical mean times to failure and repair (MTTF, MTTR)

The mean time to failure (MTTF) for 0% rain reads according to columns 2 to 4 of Table 2 evaluating equation (6) for equidistant inspection times

$$MTTF_{sim}(0\%\text{ rain}) \approx 5\,s \cdot \frac{4+1+1+2+2+1+2+2+1+1+2}{3+3+3+2} = \frac{5\,s \cdot 19}{11} = \frac{95\,s}{11} = 8.64\,s. \tag{10}$$

In a similar way we find subsequently according to columns 5 to 7,

$$MTTF_{sim}(25\%\ \text{rain}) \approx 5\ s \cdot \frac{2+1+1+2+2+1+2+1+1+1}{3+3+4} = \frac{5\ s \cdot 14}{10} = \frac{1 \cdot 7\ s}{1} = 7.00\ s. \tag{11}$$

according to columns 8 to 10,

$$MTTF_{sim}(75\%\ \text{rain}) \approx 5\ s \cdot \frac{1+1+1+1+1+1+1+2+2}{3+3+3} = \frac{5\ s \cdot 11}{10} = \frac{11\ s}{2} = 5.50\ s. \tag{12}$$

and according to the last three columns,

$$MTTF_{sim}(100\%\ \text{rain}) \approx 5\ s \cdot \frac{2+1+1+2+1+1+1+1}{3+3+2} = \frac{5\ s \cdot 10}{8} = \frac{5\ s \cdot 5}{4} = 6.25\ s. \tag{13}$$

The number of failure sequences decreases monotonously from 0% rain to 100% rain. Overall, also the $MTTF_{sim}$ decreases as the failure duration increases, however, $MTTF_{sim}(75\%\ \text{rain})$ is smaller than $MTTF_{sim}(100\%\ \text{rain})$.

The mean time to repair (MTTF) for 0% rain reads according to columns 2 to 4 of Table 2 evaluating equation (7) for equidistant inspection times

$$MTTR_{sim}(0\ \%\ \text{rain}) \approx 5\ s \cdot \frac{1+1+4+3+1+1+1+2+1+3}{3+3+4} = \frac{5\ s \cdot 18}{10} = \frac{18\ s}{2} = 9.00\ s. \tag{14}$$

In a similar way we find subsequently according to columns 5 to 7,

$$MTTR_{sim}(25\%\ \text{rain}) \approx 5\ s \cdot \frac{3+5+2+2+2+1+4+3+1}{3+3+3} = \frac{5\ s \cdot 23}{9} = \frac{115\ s}{9} = 12.78\ s. \tag{15}$$

according to columns 8 to 10,

$$MTTR_{sim}(75\%\ \text{rain}) \approx 5\ s \cdot \frac{4+4+2+4+1+3+1+2+3+1}{3+3+4} = \frac{5\ s \cdot 25}{10} = \frac{25\ s}{2} = 12.50\ s. \tag{16}$$

and according to the last three columns,

$$MTTR_{sim}(75\%\ \text{rain}) \approx 5\ s \cdot \frac{5+5+5+1+1+4+6}{3+3+1} = \frac{5\ s \cdot 27}{7} = \frac{135\ s}{7} = 19.26\ s. \tag{17}$$

Overall, the number of repair intervals decreases from 0% rain to 100% rain as well the $MTTR_{sim}$ increases as the non-operational intervals increase on average. Note that $MTTR_{sim}(25\%\ \text{rain})$ is slightly greater than $MTTR_{sim}(75\%\ \text{rain})$.

Using a discrete probability density an alternative way of computing $MTTR_{sim}$ is as follows. First, observe that there are 6 sequences of length 5 s, 1 sequences of length 10 s, 2 failure sequences of length 15 s, 1 sequence of length 20 s. Then the total number of failure sequences of lengths $t_1 = 5\ s, t_2 = 10\ s, \ldots$ is given by

$$N_{tot}(0\%\ \text{rain}) = \sum_{i=1}^{\infty} N_{sequence}(t_i) = 6 + 1 + 2 + 1 = 10. \tag{18}$$

Now the normalization condition of the length of failure sequence distribution reads using a Riemann sum

$$a\ \Delta t\ \sum_{i=1}^{\infty} N_{sequence}(t_i) = 1, \tag{19}$$

which is used to define the normalized ($\sum_{i=1}^{\infty} \widetilde{N}_{sequence}(t_i)\ \Delta t = 1$) failure sequence length (downtime length distribution or repair time distribution)

$$\widetilde{N}_{sequence}(t) = \text{a}\ N_{sequence}(t_i). \tag{20}$$

Now the mean time to repair can be defined as the expectation value or first moment (see, e.g. (Skartlien and Oyehaug 2005) for similar expectations from discrete probability distributions) of the normalized discrete failure sequence length distribution

$$\begin{aligned} \overline{T}_{repair} = E_{discrete}[\text{t}] = \ & \sum_{i=1}^{\infty} \widetilde{N}_{sequence}(t_i)\ t_i\ \Delta\text{t} = \text{a}\ \sum_{i=1}^{\infty} N_{sequence}(t_i)\ t_i\ \Delta t \\ &= \frac{1}{\Delta t \sum_{i=1}^{\infty} N_{sequence}(t_i)} \sum_{i=1}^{\infty} N_{sequence}(t_i)\ t_i\ \Delta t \\ &= \frac{1}{\Delta t\ N_{tot}} \sum_{i=1}^{\infty} N_{sequence}(t_i)\ t_i\ \Delta t = \frac{1}{\text{N}_{\text{tot}}} \sum_{i=1}^{\infty} N_{sequence}(t_i)\ t_i\ . \end{aligned} \tag{21}$$

Note that the last line of (21) corresponds to the expression (7) in case the observation of the component status starts with operational subsystem. For example, the second last expression in last row of (22) reads, using data of Table 2,

$$\begin{aligned} \overline{T}_{repair}(0\%\ \text{rain}) &= \frac{1}{5\ s}\left(\frac{6 \cdot 5\ s}{10} + \frac{1 \cdot 10\ s}{10} + \frac{2 \cdot 15\ s}{10} + \frac{1 \cdot 15\ s}{10}\right)\ 5\ \text{s} \\ &= \left(\frac{30\ s}{10} + \frac{10\ s}{10} + \frac{30\ s}{10} + \frac{15\ s}{10}\right) = \frac{85}{10}\ \text{s} = 8.5\ \text{s}. \end{aligned} \tag{22}$$

which is consistent with the simpler mean value expression of equation (14).

4.3. Asymptotic probability of being in an operational and in a failed sate

From the empirical MTTFs in equations (10) to (13) and the empirical MTTRs in (14) to (17) we determine the asymptotic probability of being in an operational and in a failed sate using (9). The results are summarized in Table 3. It shows that on average $p_0(\infty)$ decreases and $p_1(\infty)$ increases with increasing rain intensities. It is interesting to observe that even if none of the rates or MTTX increase or decrease monotonously with respect to increasing rain intensities, the asymptotic probabilities for operation and fail states as well as the failure probability in observation interval as introduced in (23) below do.

Table 3. Failure and repair quantities for AD lane detection dependence on rain intensity: Failure and repair (or recovery) rate per lane detection system belonging to a single car, mean time to failure (MTTF), to repair (MTTR), asymptotic operational $p_0(\infty)$ and failure probability $p_1(\infty)$ and probability of failure in observation interval for rain intensities 0%, 25%, 75% and 100% as computed from data of Table 2.

Rain intensity [%]	Failure rate λ [1/s]	Repair rate μ [1/s]	MTTF [s]	MTTR [s]	Asymptotic probability of being in operational state $p_0(\infty)$ [-]	Asymptotic probability of being in failed state $p_1(\infty)$ [-]	Failure probability in observation interval
0	0.116	0.111	8.64	9.00	0.490	0.510	0.500
25	0.143	0.078	7.00	12.8	0.354	0.646	0.638
75	0.182	0.080	5.50	12.5	0.306	0.694	0.694
100	0.160	0.052	6.25	19.3	0.245	0.755	0.750

4.4. Failure and repair rates from empirical meant times to failure and repair (MTTF, MTTR)

The observation that the failure rate is not increasing monotonously (or equivalently the MTTF is not decreasing monotonously) arises the question if alternative failure rate definitions can be introduced that take better into account that the AD lane detection system fails more often in case of strong rain. To this end in section 4.3 different failure rate definitions are defined in Table 4. Table 4 lists the various definitions of failure rates used and describes how the quantities are computed, further can be found in (Padariya 2024).

Table 4. Failure rate per time definitions for AD lane detection system. The table gives short name, short description and how to determine the quantity from observational data in case of equidistant health status inspection of lane detection as given in the example Table 2.

Short name	Description	Example computation
Failure probability in total observation time per time	Determine total length of intervals with failure and divide twice by total observation interval length	See text along with equation (23) and its discussion
Failure rate for the failure observations at inspection	Number of observed failures at inspection divided by observation time	Number of **black** crosses in Table 2 divided by 180 s
Failure rate for the failure sequences observed	Number of failure sequences without interruption divided by time interval	As above using number of **red** crosses.
Failure rate for the failure sequences with up to 3 crosses	As above but start to count as new failure sequence if longer than 3 observations	As above using number of **blue** crosses.
Failure rate for the failure sequences with up to 2 crosses	As above but count as new sequence as soon as longer than 2 observations	As above using number of **violet** crosses.
Failure rate for the failure sequences with 2 crosses	As above but do not count single remaining failure observations, e.g. failure sequence of 3 observations is counted as 1 failure sequence	As above using number of **orange** crosses.

The failure probability (in observation time) per observation time of the second row of Table 4 is defined as

$$f = \frac{\text{failure probability in observation time}}{\text{observation time}} \tag{23}$$

$$= \frac{\frac{1}{\text{observation time}} \sum_{i=0}^{N_{inspec}} (\text{failure at inspection i})_{lb} \cdot (\text{length of inspection interval } i)}{\text{observation time}}$$

$$= \frac{\sum_{i=0}^{N_{inspec}} (f_{mode}(t_i)=\text{fail})_{lb} \cdot (\text{length of } I_i)}{(t_{up}-t_{low})^2},$$

where we introduced N_{inspec} inspection intervals I_i, their lengths, start time t_{low} and end time of inspections t_{up}, and ordered inspection times $t_{low} \le t_0 < t_1 < \cdots < t_{insepc} \le l_{up}$, which are at the center or at least within the respective inspection intervals. For instance, for 0% rain we find with the help of the second to the fourth column of Table 2, see also corresponding entry in Table 4.

$$\text{f(0\% rain)} = \frac{\sum_{i=0}^{N_{inspec}} (f_{mode}(t_i)=\text{fail})_{lb} \cdot (\text{length of } I_i)}{(t_{up}-t_{low})^2} \tag{24}$$

$$= \frac{0{\cdot}5 \text{ s}+0{\cdot}5 \text{ s}+0{\cdot}5 \text{ s}+0{\cdot}5 \text{ s}+1{\cdot}5 \text{ s}....+1{\cdot}5 \text{ s}+0{\cdot}5 \text{ s}+ 0{\cdot}5 \text{ s}}{(180 \text{ s}-0 \text{ s})2} = \frac{90\ s}{(180 \text{ s})^2} = 2.78\text{E-}3 \text{ s}^{-1}.$$

The quantities introduced in Table 4 are computed from CARLA lane detection inspection raw data of Table 2 in Table 5. It can be seen in Table 5 that the failure probability within the observed time interval divided by the time observed, the failure rate for failure observations at inspection, the failure rate for failure sequences with up to 2 crosses (i.e. starting to count a new failure sequence if failure sequence is longer than 2 observations or 10 s), and the failure rate for failure sequences with 10 s increase monotonously as expected with higher rain intensities. However, the failure rate for the failure rate for failure sequences observed and the failure sequences with up to 3 crosses (or 15 s duration) do not increase monotonously with increasing rain intensity.

When comparing failure rate values with failure rates from MTTF computations as given in Table 3, see last line of Table 5, we observe that none of the alternative proposed definitions exhibits a similar behavior. Note that the failure rates that re-start counting failure sequences incorporate the assumption that lane detection failure becomes again critical if duration is longer than some critical duration. This assumption is not incorporated in the 2 state Markov model considering failure and repair rates used for the asymptotic operational and failure probability computations of Table 3.

Table 5. Lane detection failure rate results for different failure rate per time definitions depending on the duration of the downtime using definitions of Table 4.

	Rain intensity [%]			
Failure rate type	0	25	75	100
Failure probability over time observed [1/s]	2.78E-3	3.54E-3	3.86E-3	4.17E-3
Failure rate for failure observations at inspection [1/s]	1.00E-1	1.28E-1	1.38E-1	1.50E-1
Failure rate for failure sequences observed [1/s]	5.60E-2	5.00E-2	5.00E-2	3.80E-2
Failure rate for failure sequences with up to 3 crosses [1/s]	6.10E-2	6.10E-2	8.90E-2	6.70E-2
Failure rate for failure sequences with up to 2 crosses [1/s]	5.60E-2	6.10E-2	6.70E-2	7.30E-2
Failure rate for failure sequences with 2 crosses [1/s]	2.20E-2	2.70E-2	5.00E-2	6.20E-2
Failure rate (from MTTF computation) [1/s]	1.16E-1	1.43E-1	1.82E-1	1.60E-1

The findings imply that even simple analytical methods like Failure Mode and Effects and Diagnostics Analysis (FMEDA, e.g. (Häring 2021a)), Fault Tree Analysis (FTA, e.g. (Häring 2021b)), Hazard Analysis (HA, e.g (Häring 2021c)), failure rate prediction (e.g. (Häring 2021d)) require as background model at least classical application domain specific constant failure rate and repair models, failure models only are not sufficient. AD simulations like CARLA offer a variety of functionalities including the modeling of subfunctions of AD including detection, classification, identification, and tracking of persons, objects and road elements, route planning, and maneuver planning. All of these functionalities operate at high resolution level regarding scenario details such as conditions of weather, daytime, road type, traffic conditions, etc. In contrast, analytical safety assessments operate at an abstract level in terms of failures per time or conditional failure rates such as failure of object detection given certain weather or daytime conditions. The approach presented shows that simulation results can be summarized in failure and repair models using constant rates only.

5. Conclusions

The evaluation of autonomous vehicles' safety is key for their use on public roads. It is difficult because of their advanced technology and complexity, still limited real-world usage, and the manufacturers' reluctance to share failure data and their assessment. This motivates ongoing research efforts regarding safety evaluation processes and methods. The paper uses CARLA simulation to estimate failure and repair or recovery rates for the sample AD autonomous subsystem lane detection.

Using the CARLA simulator, it was possible to create realistic driving situations for highway scenarios that were altered and recreated in different scenario variations. The focus was on the influence of rain/precipitation intensity while assuming no fog but allowing for different times of the day and sun position angles. The CARLA simulator generated a driving route through a selected city map (Town05) for a given rain percentage (0% to 100%) and with fog density zero. CARLA varied itself time of the day, spawned vehicles for a set number of vehicles in the scenario (100 vehicles in total), number of pedestrians in the scenario (70 pedestrians in total), and some more settings (see more settings in Table 1).

The simulator covered 30 minutes but for the manual inspection of data for evaluation only 3 minutes were selected due to necessary effort. Every 5 seconds the video was inspected (at 0 s, 5, s, …, 180 s) and lane detection status was assessed creating operational and fail assessments. Thus, for the 180 s driving and one rain intensity 37 inspection values were generated. In total 4 rain intensities were considered: 0%, 25%, 75% and 100%, as the change in the middle was found to be rather small. In this way in total $37 \cdot 4 = 148$ inspection values were generated.

In total 6 different types of failure rates per time were defined and evaluated for all rain intensities. The resulting failure rates showed that all failure rates increased monotonously when moving from 0%, to 25% and 75% rain intensity. However, definitions that did not account for counting more failure in case of long failure sequences generated decreasing failure rates when moving from 75% rain to 100 % rain intensity. This is interpreted as an effect of the increasing length of the failure sequences while their number decreases.

This shows that the complete modeling needs to consider both failure duration and failure repair times. They were estimated from empirical failure and repair duration times assuming constant rates for each rain intensity, i.e. exponential distributions. The interesting observation is that even if failure and repair rates themselves are not consistent, when combining them to a simple 2 state Markov model, the asymptotic probabilities of being in an operational state or in a failed state are consistent with the expectations, as they decrease and increase monotonously, respectively. They also nicely fit to the observed probability of being in a failed state and its complement. In summary, at least constant failure rate models for different rain intensities for failure and repair modelling are necessary for consistent interpretation of simulated lane detection failures within CARLA simulator.

More straightforward improvements of the present work include to consider in addition rain intensities of 50%, to reduce inspection time to the range of a fraction of seconds, e.g. 0.1 s, and to consider longer simulation times much beyond 1 h. Furthermore, the restriction to exponential distribution could be lifted, e.g. using Weibull or Pareto distributions for failure and repair or recovery modelling of lane detection. The present approach could also be applied to the effect of fog as well as to the effect of time of the day. Detection of grade of failure could be automated to replace need for human inspection, e.g. using as training data the human failure classifications. It is also worth noting that with the help of computed failure rates, the need for further resolution could be determined either directly by inspection of the magnitude of the failure rates (should be below certain thresholds) and repair rates (should be above certain thresholds), i.e. resulting subsequently in rates of the following form $\{\lambda, \mu\}$ (rain,fog,time of the day, street geometry, $etc.$).

Acknowledgements

The presented work is funded by the German BMWK project on Real Driving Validation (RDV) with Grant number 19A21051D and funding duration 2022-2025.

References

Berlincioni, L. 2022. Autonomous Driving Research with CARLA Simulator. SIGMultimedia Rec. 14(1). 8 pp, https://doi.org/10.1145/3630646.3630648.

Binas, J., Neil, D., Liu, S.-C., Delbruck, T. 2017. DDD17: End-To-End DAVIS Driving Dataset. arXiv preprint arXiv:1711.01458.

Birolini, A. 2017. Reliability Engineering: Theory and Practice, 8th edn. Springer Berlin Heidelberg; Imprint: Springer, Berlin, Heidelberg.

Breitenstein, J., Fingscheidt, T. 2022. Amodal Cityscapes: A New Dataset, its Generation, and an Amodal Semantic Segmentation Challenge Baseline. In: 2022 IEEE Intelligent Vehicles Symposium (IV), pp 1018–1025.

Caesar, H., Bankiti, V., Lang, A.H., Vora, S., Liong, V.E., Xu, Q., Krishnan, A., Pan, Y., Baldan, G., Beijbom, O. 2020. nuScenes: A Multimodal Dataset for Autonomous Driving. In: CVF (Ed.) 2020 IEEE/CVF Conference on Computer Vision and Pattern Recognition (CVPR), pp 11618–11628

CARLA. 2023. Python API - CARLA Simulator. https://carla.readthedocs.io/en/latest/python_api/. Accessed 30 November 2023.

CARLA. 2024. CARLA: Open-source simulator for autonomous driving research. https://carla.org//. Accessed 2 January 2024.

Chamain, L.D., Qi, S., Ding, Z. 2022. End-to-End Image Classification and Compression With Variational Autoencoders. IEEE Internet Things J. 9, pp 21916–21931. https://doi.org/10.1109/JIOT.2022.3182313.

Coelho, D., Oliveira, M. 2022. A Review of End-to-End Autonomous Driving in Urban Environments. IEEE Access 10, pp 75296–75311. https://doi.org/10.1109/ACCESS.2022.3192019.

Cordts, M., Omran, M., Ramos, S., Rehfeld, T., Enzweiler, M., Benenson, R., Franke, U., Roth, S., Schiele, B. 2026. The Cityscapes Dataset for Semantic Urban Scene Understanding. In: CVPR (Ed.) 2016 IEEE Conference on Computer Vision and Pattern Recognition (CVPR), pp 3213–3223.

Dosovitskiy, A., Ros, G., Codevilla, F., Lopez, A., Koltun, V. 2017. CARLA: An Open Urban Driving Simulator. In: CoRL (Ed.) 1st Conference on Robot Learning (CoRL 2017), PMLR 78, pp 1–16.

Duer, S., Woźniak, M., Paś, J., Zajkowski, K., Bernatowicz, D., Ostrowski, A., Budniak, Z. 2023. Reliability Testing of Wind Farm Devices Based on the Mean Time between Failures (MTBF). Energies 16, 1659, 16 pp, https://doi.org/10.3390/en16041659.

El-Wajeh, Y.A.M., Hatton, P.V., Lee, N.J. 2022. Unreal Engine 5 and immersive surgical training: translating advances in gaming technology into extended-reality surgical simulation training programmes. Br J Surg 109, pp 470–471. https://doi.org/10.1093/bjs/znac015.

Fenoaltea, F. 2022. Reliability Based Classification of Transitions in Complex SemiMarkov Models, KTH Royal Institute of Technology.

Finkelstein, M. 2008. Failure Rate Modelling for Reliability and Risk, 1st edn. Springer Series in Reliability Engineering. Springer London.

Geiger, A., Lenz, P., Stiller, C., Urtasun, R. 2013. Vision meets robotics: The KITTI dataset. The International Journal of Robotics Research 32, pp 1231–1237. https://doi.org/10.1177/0278364913491297.

Goble, W.M. 2010. Control systems safety evaluation and reliability, 3rd edn. ISA resources for measurement and control series. International Society of Automation, Research Triangle Park, NC.

Gupta, G., Mishra, R.P., Jain, P. 2015. Reliability analysis and identification of critical components using Markov model. In: IEEM (Ed.) IEEE International Conference on Industrial Engineering and Engineering Management (IEEM), pp 777–781.

Häring, I. 2021a. Failure Modes and Effects Analysis. In: Häring I (Ed.) Technical Safety, Reliability and Resilience: Methods and Processes, 1st edn. Springer, Singapore, pp 101–126.
Häring, I. 2021b. Fault Tree Analysis. In: Häring I (Ed.) Technical Safety, Reliability and Resilience: Methods and Processes, 1st edn. Springer Singapore, pp 71–99.
Häring, I. 2021c. Hazard Analysis. In: Häring I (Ed.) Technical Safety, Reliability and Resilience: Methods and Processes, 1st edn. Springer, Singapore, pp 127–159.
Häring, I., 2021d, Reliability Prediction. In: Häring I (Ed.) Technical Safety, Reliability and Resilience: Methods and Processes, 1st edn. Springer, Singapore, pp 161–178.
Häring, I., Lüttner, F., Frorath, A., Fehling-Kaschek, M., Ross, K., Schamm, T., Knoop, S., Schmidt, D., Schmidt, A., Ji, Y., Yang, Z., Rupalla, A., Hantschel, F., Frey, M., Wiechowski, N., Schyr, C., et al. 2021. Framework for safety assessment of autonomous driving functions up to SAE level 5 by self-learning iteratively improving control loops between development, safety and field life cycle phases. In: IEEE ICCP (Ed.) 2021 IEEE 17th International Conference on Intelligent Computer Communication and Processing (ICCP), pp 33–40.
Häring, I., Satsrisakul, Y., Finger, J., Vogelbacher, G., Köpke, C., Höflinger, F. 2022. Advanced Markov modeling and simulation for safety analysis of autonomous driving functions up to SAE 5 for development, approval and main inspection. In: ESREL 2022 (Ed.) Proceedings of 32nd European Safety and Reliability Conference, pp 104–111.
Häring, I., Nikhilesh, S., Teo, P.-W., Vogelbacher, G., Alexander, R., Asihvarya, J.K., Mayur, D., Sunil, M., Konstantin K, et al. 2023a Dynamically resolving and abstracting Markov models for system resilience analysis. In: Brito MP, Aven T, Baraldi P, Čepin M, Zio E (eds) The 33rd European Safety and Reliability Conference (ESREL 2023), The Future of Safety in the Reconnected World, pp 241–248.
Häring, I., Sunil, M.K.R., Teo, P.-W., Mayur, D., Nikhilesh, S., Jörg, F., Georg, V., Fabian, H., Aishavarja, J.K., Alexander, R., Konstantin, K. 2023b. Overall Markov diagram design and simulation example for scalable safety analysis of autonomous vehicles. In: Brito MP, Aven T, Baraldi P, Čepin M, Zio E (eds) The 33rd European Safety and Reliability Conference (ESREL 2023), The Future of Safety in the Reconnected World, pp 2261–2268.
Häring, I., Sandela, N., Padariya, R., Vogelbacher, G., Höflinger, F., Richter, A., Finger, J., Jain, A.K., Kirchheim, K. 2024. Accepted Paper: Failure rates per time for autonomous driving safety assessment from CARLA simulation. In: ESREL (Ed.) 34-th European Safety and Reliability Conference, Advances in Reliability, Safety and Security, 10 pp.
Horeis, T.F., Kain, T., Muller, J.-S., Plinke, F., Heinrich, J., Wesche, M., Decke, H. 2020. A Reliability Engineering Based Approach to Model Complex and Dynamic Autonomous Systems. In: MetroCAD (Ed.) 2020 International Conference on Connected and Autonomous Driving (MetroCAD), pp 76–84.
Hu, Y., Binas, J., Neil, D., Liu, S.-C., Delbruck, T. 2020. DDD20 End-to-End Event Camera Driving Dataset: Fusing Frames and Events with Deep Learning for Improved Steering Prediction. In: ITSC (Ed.) International Conference on Intelligent Transportation, pp 1–6.
Huang, W., Wang, K., Lv, Y., Zhu, F. 2016. Autonomous vehicles testing methods review. In: ITCS (Ed.) 19th International Conference on Intelligent Transportation Systems, Rio de Janeiro, Brazil, pp 163–168.
Malik, S., Khan, M.A., El-Sayed, H. 2022. CARLA: Car Learning to Act - An Inside Out. Procedia Computer Science 198, pp 742–749. https://doi.org/10.1016/j.procs.2021.12.316.
Mattsson, O. 2020. Quantified safety modeling of autonomous systems with hierarchical semi-Markov processes, KTH Royal Institute of Technology.
Musiol, G., Mühlig, H., Semendjaev, K.A., Bronštejn, I.N. 1995. Taschenbuch der Mathematik, 2nd edn. Deutsch, Thun, Frankfurt a.M.
Nyberg, M. 2018. Safety analysis of autonomous driving using semi-Markov processes, In: ESREL 2008 Proceedings, Haugen et al. (Ed.), pp 781–788. https://doi.org/10.1201/9781351174664, https://www.taylorfrancis.com/books/e/9781351174664. Accessed 17 October 2019
Padariya, R. 2024. Failure rate estimation of lane detection from CARLA simulation for Markov model safety assessment of autonomous driving functions. Master Thesis, Fraunhofer EMI; Westsächsische Hochschule Zwickau.
Pouya, P., Madni, A.M. 2021. Expandable-Partially Observable Markov Decision-Process Framework for Modeling and Analysis of Autonomous Vehicle Behavior. IEEE Systems Journal 15, pp 3714–3725. https://doi.org/10.1109/JSYST.2020.3010473.
Pouya, P., Madni, A.M. 2022. Probabilistic System Modeling for Complex Systems Operating in Uncertain Environments. In: Madni AM, Boehm B, Erwin D, Moghaddam M, Sievers M, Wheaton M (Eds.) Recent Trends and Advances in Model Based Systems Engineering. Springer International Publishing, Cham, pp 113–127.
Puig Walz, T., Mopuru, S.K.R., Vogelbacher, G., Richter, A., Höflinger, F., Häring I, Finger J, Stolz A. 2023. Markov Modelling for Autonomous Vehicle Safety Assessment: Numerical Modularization to Avoid System State-Explosion. In: IEEE ITSC (Ed.) 26th IEEE International Conference on Intelligent Transportation Systems ITSC 2023, pp 4881-4886, https://doi.org/10.1109/ITSC57777.2023.10421943.
Rausand, M. 2011. Risk Assessment: Theory, Methods, and Applications, 1st edn. Wiley, Hoboken, New Jersey.
Rausand, M. 2014. Reliability of safety-critical systems: Theory and applications. Wiley, Hoboken, New Jersey.
Rausand, M., Haugen, S. 2020. Risk assessment: Theory, methods, and applications. Wiley series in statistics in practice. John Wiley & Sons, Hoboken, NJ
Richter, A., Puig Walz, T., Dhanani, M., Häring, I., Vogelbacher, G., Höflinger, F., Finger, J., Stolz, A. 2023. Components and Their Failure Rates in Autonomous Driving. In: Brito MP, Aven T, Baraldi P, Čepin M, Zio E (eds) The 33rd European Safety and Reliability Conference (ESREL 2023), The Future of Safety in the Reconnected World, pp 233–240.
Riedmaier, S., Ponn, T., Ludwig, D., Schick, B., Diermeyer, F. 2020. Survey on Scenario-Based Safety Assessment of Automated Vehicles. IEEE Access 8, pp 87456–87477. https://doi.org/10.1109/ACCESS.2020.2993730.
Rinaldo, R.C., Horeis, T.F. 2020. A Hybrid Model for Safety and Security Assessment of Autonomous Vehicles. In: CSCS (Ed.) Proceedings of the 4th ACM Computer Science in Cars Symposium (CSCS), pp 1–10.
Rosique, F., Navarro, P.J., Fernández, C., Padilla, A. 2019. A Systematic Review of Perception System and Simulators for Autonomous Vehicles Research. Sensors (Basel) 19(3), 648, 29 pp.. https://doi.org/10.3390/s19030648
Satsrisakul, Y. 2018. Quantitative probabilistic safety assessment of autonomous car functions with Markov models. Master Thesis, Universität Freiburg.
Skartlien, R., Oyehaug, L. 2005. Quantization Error and Resolution in Ensemble Averaged Data With Noise. IEEE Trans. Instrum. Meas. 54, pp. 1303–1312. https://doi.org/10.1109/TIM.2005.847116.
Verma, A.K., Ajit, S., Karanki, D.R. 2016. Reliability and Safety Engineering. Springer, London.
Xu, H., Gao, Y., Yu, F., Darrell, T. 2017. End-to-End Learning of Driving Models from Large-Scale Video Datasets. In: IEEE Conference on Computer Vision and Pattern Recognition (CVPR), pp 3530–3538.
Zhu, J., Ma., Y., Lou, Y. 2022. Multi-vehicle interaction safety of connected automated vehicles in merging area: A real-time risk assessment approach. Accid Anal Prev 166,106546, 14 pp. https://doi.org/10.1016/j.aap.2021.106546.